A Fully Integrated Nanosystem of Semiconductor Nanowires for Direct Solar Water Splitting

Chong Liu,[†,§] Jinyao Tang,[†] Hao Ming Chen,[†] Bin Liu,[†] and Peidong Yang*,[†,‡,§]

[†]Department of Chemistry and [‡]Department of Materials Science and Engineering, University of California, Berkeley, California 94720, United States

[§]Materials Sciences Division, Lawrence Berkeley National Laboratory, Berkeley, California 94720, United States

S Supporting Information

ABSTRACT: Artificial photosynthesis, the biomimetic approach to converting sunlight's energy directly into chemical fuels, aims to imitate nature by using an integrated system of nanostructures, each of which plays a specific role in the sunlight-to-fuel conversion process. Here we describe a fully integrated system of nanoscale photoelectrodes assembled from inorganic nanowires for direct solar water splitting. Similar to the photosynthetic system in a chloroplast, the artificial photosynthetic system comprises two semiconductor light absorbers with large surface area, an interfacial layer for charge transport, and spatially separated cocatalysts to facilitate the water reduction and oxidation. Under simulated sunlight, a 0.12% solar-to-fuel conversion efficiency is achieved, which is comparable to that of natural photosynthesis. The result demonstrates the possibility of integrating material components into a functional system that mimics the nanoscopic integration in chloroplasts. It also provides a conceptual blueprint of modular design that allows incorporation of newly discovered components for improved performance.

KEYWORDS: Artificial photosynthesis, water splitting, nanowire-based heterostructure
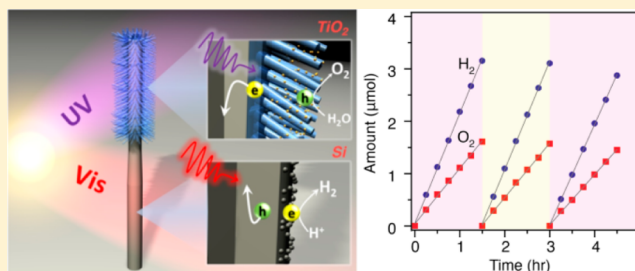
In natural photosynthesis the energy of absorbed sunlight produces energized carriers that execute chemical reactions in separate regions of the chloroplast. The electrons used to produce NADPH are excited via the "Z-scheme" of light-absorbing photosystems I and II.[1,2] The energy of the photoexcited charge carriers is then used to overcome the thermodynamic barrier and to provide any kinetic overpotential needed to drive the photosynthetic reactions. Compared to the excitation of a single light absorber, excitation of the two light absorbers, or a "Z-scheme" system, allows capture of lower energy photons and thus a larger part of the solar spectrum,[3] which can potentially lead to a higher efficiency.[4] Moreover, photosystems I and II are arranged side by side on the thylakoid membrane with the electron transport chain between them for efficient charge transfer. In addition, the spatial separation of the reduction and oxidation catalytic centers minimizes the undesirable back-reaction of the photosynthetic products. This careful arrangement of photosynthetic constituents results in a fully integrated system that facilitates conversion of solar energy into chemical fuels.[5] The average rate of energy captured by this photosynthetic process approaches 130 terawatts, about six times larger than the current worldwide power consumption.[1,2]

The same concept of an integrated system of nanostructures can be applied to artificial photosynthesis.[6−9] A general path for mimicking natural photosynthesis is to generate O_2 and H_2 separately via the "Z-scheme"[10] using two inorganic semiconductors loaded with cocatalysts. Upon exposure to light, the minority carriers in the two semiconductors will be used to carry out the individual half reactions, while the majority carriers recombine at an ohmic contact between the materials.[11−13] Such an ohmic contact is the inorganic analogue of the electron transport chain in a chloroplast. Previous studies of solar water splitting without any applied bias employed either electrode-based macroscopic devices[10,14−18] or a mixture of two semiconductor powders.[18,19] Here we demonstrate a fully integrated functional nanosystem for direct solar water splitting, in which all of the individual components, for example, two nanowire photoelectrodes with large surface area, an ohmic contact, and two cocatalysts, are carefully positioned in order to maximize the energy conversion efficiency. Such a modular approach demonstrates system-level materials design and integration[20] at the nanoscale for efficient and cost-effective solar-to-fuel conversion.

A model "Z-scheme" system with two light-absorbing materials is chosen here to demonstrate the capability of an integrated nanostructure to use sunlight to split water.[13] Earth-abundant and stable semiconductors, silicon (Si) and titanium dioxide (TiO_2), were chosen as the hydrogen-generating photocathode and oxygen-generating photoanode, respectively (Figure 1). Moreover the nanowire morphology of both
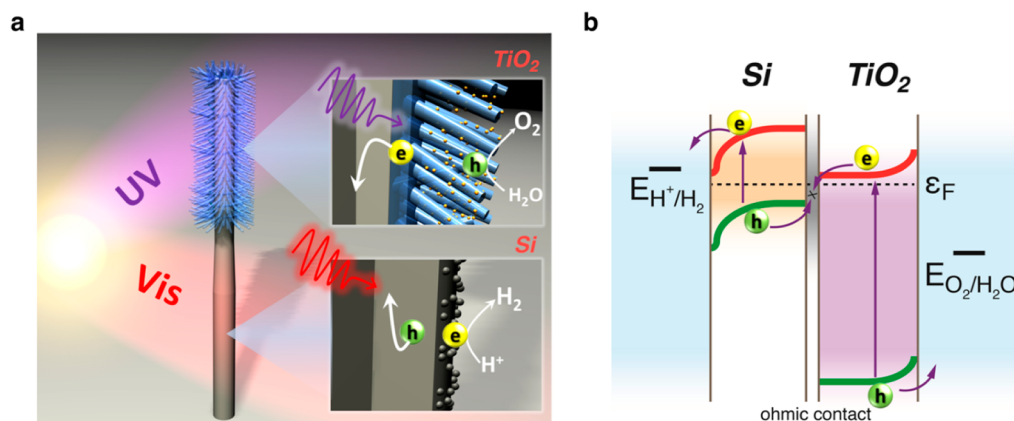
Figure 1. Schematics of the asymmetric nanoscale tree-like heterostructures used for solar-driven water splitting. a, Structural schematics of the nanotree heterostructure. The small diameter TiO_2 nanowires (blue) were grown on the upper half of a Si nanowire (gray), and the two semiconductors absorb different regions of the solar spectrum. The two insets display the photoexcited electron−hole pairs that are separated at the semiconductor-electrolyte interface to carry out water splitting with the help of cocatalysts (yellow and gray dots on the surface). b, Energy band diagram of the nanotree heterostructure for solar-driven water splitting. The photogenerated electrons in Si and holes in TiO_2 move to the surface to perform water splitting, while the holes in Si and electrons in TiO_2 recombine at the ohmic contact between the two semiconductors.

materials was applied here because of its large surface area and the shorter distances that carriers must travel to reach the semiconductor−electrolyte surface.[21] Upon illumination photoexcited electron−hole pairs are generated in Si and TiO_2, which absorb different regions of the solar spectrum. Because of the band-bending at the semiconductor−electrolyte interfaces[7] (Figure 1b), the photogenerated electrons in the Si nanowires migrate to the surface and reduce protons to generate H_2; meanwhile the photogenerated holes in the TiO_2 nanowires oxidize water to evolve O_2. The holes from Si and electrons from TiO_2 recombine at the ohmic contact, completing the relay of the "Z-scheme",[10,13] similar to that of natural photosynthesis. Owing to the difference of the two materials in catalytic and electrical transport properties, a nanoscale tree-like light-harvesting architecture is employed to maximize the performance (Figure 1a). As compared to Si nanowires, TiO_2 nanowires with smaller diameters and higher surface area are preferred because of TiO_2's shorter carrier diffusion length and slower O_2 evolution kinetics.[22] An ohmic contact was created between the Si/TiO_2 interface where majority carriers can recombine. Cocatalysts for both reactions were loaded to reduce the reactions' overpotential. The overall system resembles a nanoscale tree in which the Si nanowire serves as the trunk and the TiO_2 nanowires as the branches (Figure 1a). Such a nanotree system possesses large surface area that is favorable for catalytic reactions. At the same time the spatially separated photoelectrodes with a local ohmic contact help to segregate the products to mitigate back-reactions.[11] This nanoscale tree-like design is in principle applicable for other "Z-scheme" materials in solar-to-fuel conversion (Supporting Information), and the combination of Si and TiO_2 is demonstrated here as a proof of concept.

To realize this nanoscale tree-like architecture for artificial photosynthesis, we started by optimizing the individual components of the integrated nanosystem. Substrates with highly ordered arrays of Si nanowires 800 nm in diameter were tested as H_2-generating photocathodes. For O_2 evolution, the photoanodes consisted of single-crystalline rutile TiO_2 nanowires with diameters about 80−100 nm made using hydrothermal synthesis[23] (Figure 2a). Both Si[24−26] and TiO_2[6,27,28] nanowires have been well-studied as model systems for H_2 and
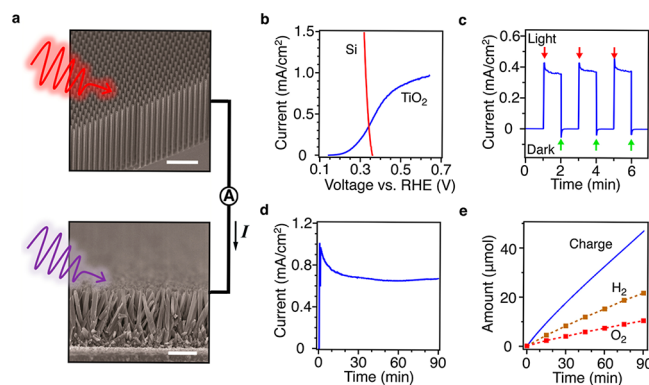

Figure 2. Optimized Si and TiO_2 nanowire photoelectrodes. a, SEM characterization of Si (top) and TiO_2 (bottom) nanowire electrodes. Nanowires of different length scales for the two semiconductors are shown. When the two semiconductor nanowire electrodes were electrically connected, immersed in water, and illuminated, a nonzero photocurrent flowed from TiO_2 to Si to carry out the water-splitting reaction. b, Photocurrent density (mA/cm^2) of Si and TiO_2 nanowires in 0.5 M H_2SO_4 solution versus the applied voltage (V) referenced to a reversible hydrogen electrode (RHE). Simulated one-sun illumination was used, and the absolute value of the photocurrent density is shown here. c, Current density (mA/cm^2) of externally short-circuited Si and TiO_2 nanowire photoelectrodes under the same conditions as b but using chopped light exposure. The measurement scheme is shown in a. d, Photocurrent measurement to test the stability of the short-circuited nanowire photoelectrodes as shown in a, under simulated three-sun illumination. e, Comparison of the evolved H_2 and O_2 gases and the charge through the circuit in d; the ratio close to 4:2:1 for charge, H_2, and O_2 proves water splitting with few losses. The scale bars in a are 10 μm (top) and 1 μm (bottom).

O_2 evolution, but they usually are tested under aqueous electrolytes of different pH for material stability and optimal performance. In addition the cocatalyst used in one half-reaction may either cross-contaminate the other cocatalyst or induce the back-reaction of the other half reaction.[19,29] In this work Si nanowire photocathodes loaded with platinum nanoparticles and TiO_2 nanowire photoanodes loaded with iridium oxide nanoparticles were tested to ensure they could function in acidic electrolyte together (Supporting Informa-
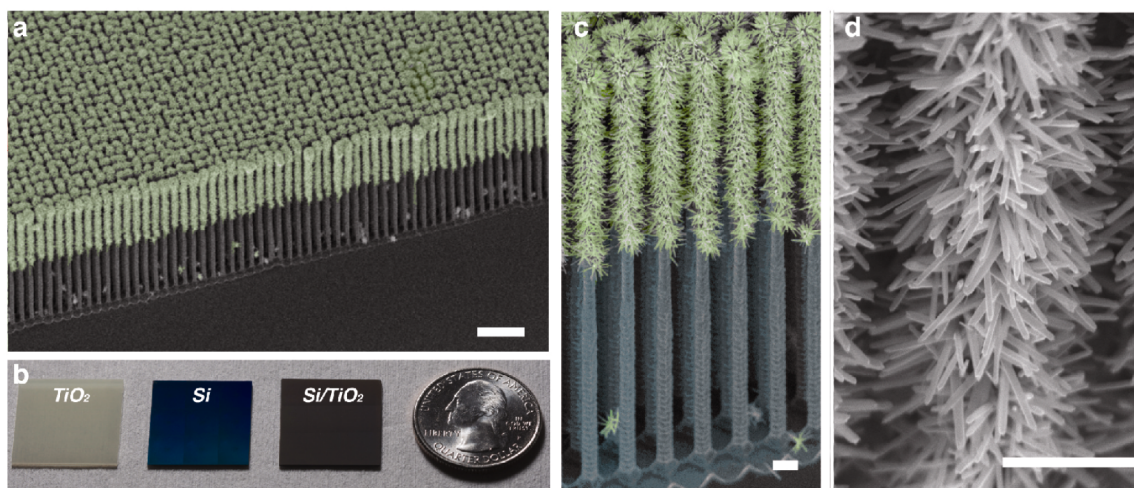
Figure 3. Structural characterization of the nanotree heterostructures. a, False-colored, large-scale SEM image of a Si/TiO$_2$ nanotree array. b, Comparison of the optical images of a TiO$_2$ nanowire substrate, a Si nanowire substrate, and a Si/TiO$_2$ nanotree substrate. c, SEM image of the details of a nanotree heterostructure. d, Magnified SEM image showing the large surface area of the TiO$_2$ segment used for water oxidation. The scale bars are 10 μm (a) and 1 μm (c, d).

tion). The optimized $J-V$ photocurrent data of both Si and TiO$_2$ nanowire photoelectrodes under simulated sunlight are plotted in Figure 2b. A current density intersection of 0.35 mA/cm^2 suggests a non-zero current flow under illumination when the Si nanowire photocathode and TiO$_2$ nanowire photoanode are directly linked together. This result is confirmed by the system's transient current response under chopped illumination (Figure 2c), implying that solar-driven water splitting without applied bias is possible for Si and TiO$_2$ nanowires when they are externally linked.

Prolonged testing of the two illuminated nanowire photoelectrodes under short-circuit conditions was also performed. Figure 2d shows that the photocurrent first decreased and then stabilized at 70% of its original performance, rendering a stabilized photocurrent of about 0.7 mA/cm^2 under simulated three-sun illumination. Under illumination, gas bubbles were evolved from the surface of both electrodes; gas chromatography measured a stoichiometric 2:1 hydrogen-to-oxygen ratio, as is expected for water splitting (Figure 2e). Moreover, comparison of the quantities of gases produced and the amount of charge that passed through the circuit shows that these nanowire electrodes exhibit a 91% charge-to-chemical Faradic efficiency.

To realize overall water splitting within an integrated nanosystem, we synthesized the nanotree heterostructure that combines the optimized photocathode and photoanode (Supporting Information). Figure 3a shows a scanning electron microscope (SEM) image of a large area of the substrate that contains many nanotree heterostructures with Si nanowire trunks and TiO$_2$ nanowire branches, that is, an artificial forest. We prepared Si nanowire arrays by reactive ion etching (RIE)[26] since it is readily available for wafer-scale fabrication, but other synthetic methods, for example, chemical vapor deposition[24] or electroless etching,[25] can also be used. As shown in Figure 3b, uniform and large-scale arrays of nanotree heterostructures are synthesized. The color of the nanotree array combines the white scattering of TiO$_2$ nanowires and the visible-light absorption of the silicon nanowire array. A closer examination of an individual nanotree (Figure 3c) shows a core−shell heterostructure with the photoanode of TiO$_2$ nanowires on the top and the photocathode of Si nanowires on the bottom. The

high surface area of the TiO$_2$ nanowires (Figure 3d) provides abundant reactive sites for the sluggish O$_2$ evolution. The Si nanowire embedded underneath the TiO$_2$ nanowire photoanode provides an ohmic contact for recombination of majority carriers and serves as a charge collector (Supporting Information), which takes advantage of the high carrier mobility of single-crystalline Si nanowires. As a fully integrated nanosystem, the entire nanotree heterostructure captures many of the essential features in natural photosynthesis.

Solar-driven water splitting without any applied bias is achieved under simulated sunlight using the nanotree heterostructures. Figure 4a displays the evolution of H$_2$ and
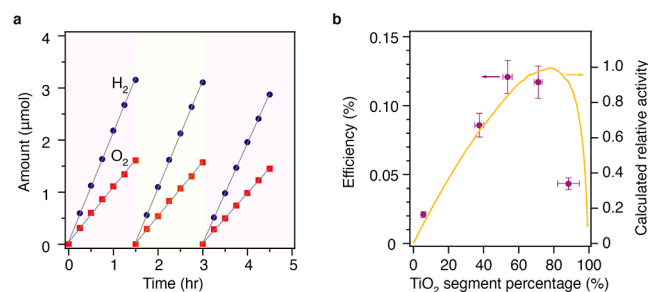

Figure 4. Solar-driven water splitting using nanotree heterostructures. a, The evolution of H$_2$ and O$_2$ gases measured by gas chromatography under simulated sunlight of 150 mW/cm^2 (1.5 suns). Nanotree heterostructures were dispersed in 0.5 M H$_2$SO$_4$ solution. After every 90 min of measurement, the gas in the reactor was purged and refilled with helium. The 2:1 ratio of H$_2$ versus O$_2$ confirmed the water-splitting reaction. b, Measured energy conversion efficiency of suspensions of nanotree heterostructures (left axis) with different percentages of TiO$_2$ covering the Si nanowires. The estimation for the normalized relative photoactivity of the nanotrees (right axis) is displayed for comparison (yellow curve).

O$_2$ gases from the Si/TiO$_2$ nanotree heterostructures dispersed in electrolyte. The 2:1 stoichiometry between H$_2$ and O$_2$ confirms the water-splitting photoactivity, and the linear increase of gas concentrations (2.1 and 1.1 μmol/h for H$_2$ and O$_2$ from 2.4 mg of nanotree heterostructures) reveals stable catalytic performance. Since no direct water splitting is

observed from dispersions of Si nanowires, TiO_2 nanowires, or their mixture (Supporting Information), the solar-driven water splitting does result specifically from the integrated design. The nanotree heterostructure displayed much higher photoactivity than the configuration where a TiO_2 thin-film is partially deposited onto Si nanowire, suggesting that the structural features for our nanoscale-tree architectrure are essential due to the vastly different optical and electrical properties of two materials used in this study (Supporting Information). Additionally, system-level optimization[20] or the nanotree heterostructure is carried out. Because of the current-matching requirement in a "Z-scheme" system, the overall rate of water splitting is limited by the photoelectrode that produces the smaller photocurrent output.[8] By varying the percentage of the nanotree that is covered in TiO_2 nanowires, an optimized water-splitting photoactivity can be found. Figure 4b compares the experimental results of nanotree water splitting activity at different TiO_2 percentages (Supporting Information), with an estimation based on the $J-V$ data of the separate Si and TiO_2 nanowire photoelectrodes in Figure 2. As expected, both data sets show the best performance from a geometry in which TiO_2 is 50−80% of the heterostructure's total length. The optimized nanotree geometry allows these heterostuctures to reach an energy conversion efficiency of 0.12% under simulated sunlight, which is comparable to that of photosynthesis in plants.[2,3] The weight-normalized photoactivity of these nanotree heterostructures (about 875 μmol/h H_2 for 1 g of material) is higher than that for both electrode and powder approaches (Supporting Information), demonstrating the importance of overall nanosystem design and interface optimization. Future improvements in the material quality and the synthetic methods, along with using earth-abundant cocatalysts,[5,26] would make this nanotree architecture more efficient and cost-effective. Also an ion-conductive membrane could be potentially incorporated between the silicon nanowires and the TiO_2 nanowires to realize macroscopic separation of H_2 and O_2.[11,12,30] These nanoscale tree-like heterostructures illustrate the feasibility of integrating individual nanoscale components into a functional system that mimics the nanoscopic integration in chloroplasts. More generally, the modular design of this overall nanosystem also provides a pathway toward better solar-to-fuel conversion efficiency as it allows newly discovered individual components to be readily plugged in.

■ ASSOCIATED CONTENT

Ⓢ Supporting Information
Detailed method for nanostructure synthesis and characterization of solar-to-fuel conversion. This material is available free of charge via the Internet at http://pubs.acs.org.

■ AUTHOR INFORMATION

Corresponding Author
*E-mail: p_yang@berkeley.edu.
Author Contributions
C.L. and J.T. contributed equally to this work.
Notes
The authors declare no competing financial interest.

■ ACKNOWLEDGMENTS

■ REFERENCES

(1) Hall, D.; Rao, K. *Photosynthesis*, 6th ed.; Cambridge University Press: New York, 1999.
(2) Barber, J. *Chem. Soc. Rev.* **2009**, *38*, 185−196.
(3) Blankenship, R. E.; Tiede, D. M.; Barber, J.; Brudvig, G. W.; Fleming, G.; Ghirardi, M.; Gunner, M. R.; Junge, W.; Kramer, D. M.; Melis, A.; et al. *Science* **2011**, *332*, 805−809.
(4) Bolton, J. R.; Strickler, S. J.; Connolly, J. S. *Nature* **1985**, *316*, 495−500.
(5) Nocera, D. G. The artificial leaf. *Acc. Chem. Res.* **2012**, *45*, 767−776.
(6) Fujishima, A.; Honda, K. *Nature* **1972**, *238*, 37−38.
(7) Gratzel, M. *Nature* **2001**, *414*, 338−344.
(8) Walter, M. G.; Warren, E. L.; McKone, J. R.; Boettcher, S. W.; Mi, Q.; Santori, E. A.; Lewis, N. S. *Chem. Rev.* **2011**, *110*, 6446−6473.
(9) Tachibana, Y.; Vayssieres, L.; Durrant, J. R. *Nat. Photonics* **2011**, *6*, 511−518.
(10) Nozik, A. J. *Appl. Phys. Lett.* **1976**, *29*, 150−153.
(11) Gray, H. B. *Nat. Chem.* **2009**, *1*, 7.
(12) Turner, J. *Nat. Mater.* **2008**, *7*, 770−771.
(13) Liu, C.; Hwang, Y. J.; Jeong, H. E.; Yang, P. *Nano Lett.* **2011**, *11*, 3755−3758.
(14) Reece, S. Y.; Hamel, J. A.; Sung, K.; Jarvi, T. D.; Esswein, A. J.; Pijpers, J. J. H.; Nocera, D. G. *Science* **2011**, *334*, 645−648.
(15) Kainthla, R. C.; Khan, S. U. M.; Bockris, J. O. M. *Int. J. Hydrogen Energy* **1987**, *12*, 381−392.
(16) Khaselev, O. *Science* **1998**, *280*, 425−427.
(17) Miller, E. L.; Paluselli, D.; Marsen, B.; Rocheleau, R. E. *Sol. Energy Mater. Sol. Cells* **2005**, *88*, 131−144.
(18) Kudo, A. *MRS Bull.* **2011**, *36*, 32−38.
(19) Maeda, K.; Domen, K. *J. Phys. Chem. Lett.* **2010**, *1*, 2655−2661.
(20) Yang, P.; Tarascon, J.-M. *Nat. Mater.* **2012**, *11*, 560−563.
(21) Yang, P.; Yan, R.; Fardy, M. *Nano Lett.* **2010**, *10*, 1529−1536.
(22) Foley, J. M.; Price, M. J.; Feldblyum, J. I.; Maldonado, S. *Energy Environ. Sci.* **2012**, *5*, 5203−5220.
(23) Liu, B.; Aydil, E. S. *J. Am. Chem. Soc.* **2009**, *131*, 3985−3990.
(24) Boettcher, S. W.; Warren, E. L.; Putnam, M. C.; Santori, E. A.; Turner-Evans, D.; Kelzenberg, M. D.; Walter, M. G.; McKone, J. R.; Brunschwig, B. S.; Atwater, H. A.; Lewis, N. S. *J. Am. Chem. Soc.* **2011**, *133*, 1216−1219.
(25) Yuan, G.; Aruda, K.; Zhou, S.; Levine, A.; Xie, J.; Wang, D. *Angew. Chem., Int. Ed.* **2011**, *50*, 2334−2338.
(26) Hou, Y.; Abrams, B. L.; Vesborg, P. C. K.; Björketun, M. E.; Herbst, K.; Bech, L.; Setti, A. M.; Damsgaard, C. D.; Pedersen, T.; Hansen, O. *Nat. Mater.* **2011**, *10*, 434−438.
(27) Liu, G.; Wang, L.; Yang, H. G.; Cheng, H.-M.; Lu, G. Q. *J. Mater. Chem.* **2010**, *20*, 831.
(28) Hwang, Y. J.; Hahn, C.; Liu, B.; Yang, P. *ACS Nano* **2012**, *6*, 5060−5069.
(29) Sayama, K.; Arakawa, H. *J. Chem. Soc., Faraday Trans.* **1997**, *93*, 1647−1654.
(30) Spurgeon, J. M.; Walter, M. G.; Zhou, J.; Kohl, P. A.; Lewis, N. S. *Energy Environ. Sci.* **2011**, *4*, 1772.

■ NOTE ADDED AFTER ASAP PUBLICATION

This paper was published ASAP on May 6, 2013 with an error in the two equations on page 9 of the Supporting Information file. The corrected version was re-posted on May 13, 2013.